# Adaptive Space-Time Finite Element and Isogeometric Analysis

Ulrich Langer

## 1 Introduction

The traditional approaches to the numerical solution of initial-boundary value problems (IBVP) for parabolic or hyperbolic Partial Differential Equations (PDEs) are based on the separation of the discretization in time and space leading to time-stepping methods; see, e.g., [20]. This separation of time and space discretizations comes along with some disadvantages with respect to parallelization and adaptivity. To overcome these disadvantages, we consider completely unstructured finite element (fe) or isogeometric (B-spline or NURBS) discretizations of the space-time cylinder and the corresponding stable space-time variational formulations of the IBVP under consideration. Unstructured space-time discretizations considerably facilitate the parallelization and the simultaneous space-time adaptivity. Moving spatial domains or interfaces can easily be treated since they are fixed in the space-time cylinder. Beside initial-boundary value problems for parabolic PDEs, we will also consider optimal control problems constrained by linear or non-linear parabolic PDEs. Here unstructured space-time methods are especially suited since the reduced optimality system couples two parabolic equations for the state and adjoint state that are forward and backward in time, respectively. In contrast to time-stepping methods, one has to solve one big linear or non-linear system of algebraic equations. Thus, the memory requirement is an issue. In this connection, adaptivity, parallelization, and matrix-free implementations are very important techniques to overcome this bottleneck. Fast parallel solvers like domain decomposition and multigrid solvers are the most important ingredients of efficient space-time methods.
This paper is partially based on joint works with Svetlana Kyas (Matculevich) and Sergey Repin on adaptive space-time IGA based on functional a posteriori error estimators [10, 11], Martin Neumüller and Andreas Schafelner on adaptive space-time

Ulrich Langer
Institute for Computational Mathematics, Johannes Kepler University Linz, Altenbergerstr. 69, A-4040 Linz, Austria, e-mail: ulanger@numa.uni-linz.ac.at

FEM [13, 14], and Olaf Steinbach, Fredi Tröltzsch and Huidong Yang on space-time FEM for optimal control problems [15, 16].

## 2 Space-Time Variational Formulations

Let us consider the parabolic IBVP, find $u$ such that

$$\partial_t u - \mathrm{div}_x(\alpha \nabla_x u) = f + \mathrm{div}_x(\mathbf{f}) \text{ in } Q,\ u = 0 \text{ on } \Sigma,\ u = u_0 := 0 \text{ on } \Sigma_0, \tag{1}$$

as a typical model problem, where $Q = \Omega \times (0,T)$, $\Sigma = \partial\Omega \times (0,T)$, $\Sigma_0 = \Omega \times \{0\}$, $\Omega \subset \mathbb{R}^d$, $d = 1, 2, 3$, denotes the spatial domain that is assumed to be bounded and Lipschitz, $T > 0$ is the terminal time, $f \in L_2(Q)$ and $\mathbf{f} \in L_2(Q)^d$ are given sources, and $\alpha \in L_\infty(Q)$ is a given uniformly bounded and positive coefficient (matrix) that may discontinuously depend on the spatial variable $x = (x_1, \ldots, x_d)$ and the time variable $t$ (non-autonomous case). The standard variational formulation of the IBVP (1) in Bochner spaces reads as follows [17]: Find $u \in U_0 := \{v \in U := \{w \in V := L_2(0,T; H^1_0(\Omega)) : \partial_t w \in V^* := L_2(0,T; H^{-1}(\Omega))\} : v = 0 \text{ on } \Sigma_0\}$ such that

$$a(u,v) = \ell(v) \quad \forall v \in V, \tag{2}$$

where the bilinear form $a(\cdot,\cdot)$ and the linear form $\ell(\cdot)$ are defined by the identities

$$a(u,v) := \int_Q [\partial_t u(x,t) v(x,t) + \alpha(x,t) \nabla_x u(x,t) \cdot \nabla_x v(x,t)]\, dQ \text{ and}$$
$$\ell(v) := \int_Q [f(x,t) v(x,t) - \mathbf{f}(x,t) \cdot \nabla_x v(x,t)]\, dQ, \text{ respectively.}$$

We note that $U = W(0,T)$ is continuously embedded into $C([0,T], L_2(\Omega))$; see [17]. Alternative space-time variational formulations of the IBVP (1) in anisotropic Sobolev spaces on $Q$ are discussed in [9]. The textbook proof of existence and uniqueness of a weak solution is based on Galerkin's method and a priori estimates; see, e.g., [17] and [9]. Alternatively one can use the Banach-Nečas-Babuška (BNB) theorem (see, e.g., [3, Theorem 2.6]) that provides sufficient and necessary conditions for the well-posedness of variational problems like (2). Indeed, Steinbach proved in [19] for $\alpha = 1$ that the bilinear form $a(\cdot,\cdot)$ fulfills the following three conditions:

(BNB1) boundedness: $|a(u,v)| \le \sqrt{2}\, \|u\|_U \|v\|_V,\ \forall u \in U_0, v \in V$,
(BNB2) inf-sup condition: $\inf_{u \in U_0 \setminus \{0\}} \sup_{v \in V \setminus \{0\}} \frac{a(u,v)}{\|u\|_U \|v\|_V} \ge 1/(2\sqrt{2})$,
(BNB3) injectivity of $A^*$: For every $v \in V \setminus \{0\}$, there exists $u \in U_0$: $a(u,v) \neq 0$,

which are sufficient and necessary for the well-posedness of (2), in other words, the operator $A : U_0 \to V^*$, defined by $a(\cdot,\cdot)$, is an isomorphism. Moreover, $\|u\|_{U_0} \le 2\sqrt{2}\, \|\ell\|_{V^*}$. The norms in the spaces $U_0$, $U$, and $V$ are defined as follows:

$$\|u\|^2_{U_0} = \|u\|^2_U := \|u\|^2_V + \|\partial_t u\|^2_{V^*} = \|\nabla_x u\|^2_{L_2(Q)} + \|\nabla_x w_u\|^2_{L_2(Q)},$$

where $w_u \in V$ such that $\int_Q \nabla_x w_u \cdot \nabla_x v \, dQ = \langle \partial_t u, v \rangle_Q$ for all $v \in V$. Here, $\langle \cdot, \cdot \rangle_Q := \langle \cdot, \cdot \rangle_{V^* \times V}$ denotes the duality product on $V^* \times V$.

In the following two sections, *maximal parabolic regularity* plays an important role when deriving locally stabilized isogeometric and finite element schemes. Let us assume that $\mathbf{f} = \mathbf{0}$ and that the coefficient $\alpha = \alpha(x,t)$ fulfills additional conditions (see, e.g., [2]) such that the solution $u \in U_0$ of (2) belongs to the space

$$H_0^{L,1}(Q) = \{v \in V : \partial_t v,\ L_x v := \mathrm{div}_x(\alpha \nabla_x u) \in L_2(Q)\}.$$

Hence, the PDE $\partial_t u - L_x u = f$ holds in $L_2(Q)$. The maximal parabolic regularity even remains true for inhomogeneous initial data $u_0 \in H_0^1(\Omega)$. We also refer the reader to the classical textbook [9], where the case $\alpha = 1$ was considered.

## 3 Space-Time Isogeometric Analysis

Let us assume that $\mathbf{f} = \mathbf{0}$ and that $\alpha$ fulfills conditions such that maximal parabolic regularity holds, i.e. the parabolic PDE (1) can be treated in $L_2(Q)$. The time variable $t$ can be considered as just another variable, say, $x_{d+1}$, and the term $\partial_t u$ can be viewed as convection in the direction $x_{d+1}$. Thus, we can multiply the parabolic PDE (1) by a time-upwind test function $v_h + \lambda \partial_t v_h$ in order to derive stable discrete schemes, where $v_h$ is a test function from some finite-dimensional test space $V_{0h}$, and $\lambda \geq 0$ is an appropriately chosen scaling parameter. This choice of test functions is motivated by the famous SUPG method, introduced by Hughes and Brooks for constructing stable fe schemes for stationary convection-diffusion problems [4], and which was later used by Johnson and Saranen [7] for transient problems; see also [6] for the related Galerkin Least-Squares finite element methods. Instead of fe spaces $V_{0h}$, we can also use IGA (B-splines, NURBS) spaces that have some advantages over the more classical fe spaces; see [5] where IGA was introduced. In particular, in the single patch case, one can easily construct IGA spaces $V_{0h} \subset C^{k-1}(\overline{Q})$ of $(k-1)$-times continuously differentiable B-splines of underlaying polynomial degree $k$. These B-splines of highest smoothness have asymptotically the best approximation properties per degree of freedom. In [12], we used such IGA spaces to derive stable space-time IGA schemes provided that $\lambda = \theta h$ with a fixed constant $\theta > 0$, where $h$ denotes the mesh-size.

In order to construct stable adaptive space-time IGA schemes, we replaced the global scaling parameter $\lambda$ by a local scaling function $\lambda(x,t)$ that is changing on the mesh according to the local mesh sizes [10, 11]. Let us describe the construction of these locally stabilized space-time IGA more precisely. In IGA, we use the same basis functions for describing both the geometry and IGA spaces $V_{0h}$. Thus, we assume that the physical computational domain $Q = \Phi(\widehat{Q})$ is the image of the parameter domain $\widehat{Q} := (0,1)^{d+1}$ using the geometrical mapping $\Phi(\xi) = \sum_{i \in \mathcal{I}} \widehat{B}_{i,k}(\xi)\, \mathbf{P}_i$, where $\{\mathbf{P}_i\}_{i \in \mathcal{I}} \subset \mathbb{R}^{d+1}$ are the control points, and $\widehat{B}_{i,k}, i \in \mathcal{I}$, are the multivariate B-Splines or NURBS. Now we can define the finite-dimensional space

$$V_{0h} = \{v_h \in V_h : v_h = 0 \text{ on } \overline{\Sigma} \cup \overline{\Sigma}_0\} = \text{span}\{\varphi_i : i \in \mathcal{I}_0\} \tag{3}$$

by means of the same basis functions, i.e.,

$$V_h = \mathcal{S}_h^k = \mathcal{S}_{k-1,h}^k = \text{span}\{\varphi_i = \hat{\varphi}_i \circ \Phi^{-1} : i \in \mathcal{I}\},$$

where $\hat{\varphi}_i(\xi) = \widehat{B}_{i,k}(\xi)$, $i \in \mathcal{I}$. We now test the PDE $\partial_t u - L_x u = f$ restricted to a mesh element $K$ from the set of all mesh elements $\mathcal{K}_h = \{K = \Phi(\widehat{K})\}$, into which $Q$ is decomposed, by $v_h + \lambda_K \partial_t v_h$, yielding

$$\big(\partial_t u - L_x u, v_h + \lambda_K\, \partial_t v_h\big)_{L_2(K)} = (f, v_h + \lambda_K\, \partial_t v_h)_{L_2(K)} \quad \forall v_h \in V_{0h}.$$

Summing up over all $K \in \mathcal{K}_h$, and integrating by parts, we get the variational consistency identity

$$a_h(u, v_h) = \ell_h(v_h) \quad \forall v_h \in V_{0h}, \tag{4}$$

where the bilinear form and the linear form are defined by the identities

$$\begin{aligned} a_h(u, v_h) =& (\partial_t u, v_h)_{L_2(Q)} + (\alpha \nabla_x u, \nabla_x v_h)_{L_2(Q)} \\ &+ \sum_{K \in \mathcal{K}_h} \lambda_K \Big( (\partial_t u, \partial_t v_h)_{L_2(K)} - (L_x u, \partial_t v_h)_{L_2(K)} \Big) \end{aligned} \tag{5}$$

and

$$\ell_h(v_h) := (f, v_h)_{L_2(Q)} + \sum_{K \in \mathcal{K}_h} \lambda_K\, (f, \partial_t v_h)_{L_2(K)},$$

respectively. Now, the corresponding consistent IGA scheme reads as follows: Find $u_h \in V_{0h}$ such that

$$a_h(u_h, v_h) = \ell_h(v_h) \quad \forall v_h \in V_{0h}. \tag{6}$$

The following three properties are fundamental for the derivation of error estimates:

1. Galerkin orthogonality: $a_h(u - u_h, v_h) = 0 \quad \forall\, v_h \in V_{0h}$,
2. $V_{0h}$-coercivity: $a_h(v_h, v_h) \geq \mu_c \|v_h\|_h^2 \quad \forall\, v_h \in V_{0h}$,
3. Extended boundedness: $|a_h(u, v_h)| \leq \mu_b \|u\|_{h,*}\, \|v_h\|_h \quad \forall\, u \in V_{0h,*},\ v_h \in V_{0h}$,

provided that $\lambda_K = \theta_K h_K$ with $\theta_K = c_K^{-2} \overline{\alpha}_K^{-1} h_K$, where $h_K = \text{diam}(K)$ denotes the local mesh-size, $\overline{\alpha}_K$ is an upper bound of $\alpha$ on $K$, and $c_K$ is the computable constant (upper bound) in the local inverse inequality $\|\text{div}_x \nabla_x v_h\|_{L_2(K)} \leq c_K h_K^{-1} \|\nabla_x v_h\|_{L_2(K)}$. Then we get $\mu_c = 1/2$. The boundedness constant $\mu_b$ can also be computed; see [10, 11]. The norms $\|\cdot\|_h$ and $\|\cdot\|_{h,*}$ are defined as follows:

$$\|v\|_h^2 := \sum_{K \in \mathcal{K}_h} \Big[ \|\alpha^{1/2} \nabla_x v\|_{L_2(K)}^2 + \lambda_K \|\partial_t v\|_{L_2(K)}^2 \Big] + \frac{1}{2} \|v\|_{L_2(\Sigma_T)}^2, \tag{7}$$

$$\|v\|_{h,*}^2 := \|v\|_h^2 + \sum_{K \in \mathcal{K}_h} \big[ \lambda_K^{-1} \|v\|_{L_2(K)}^2 + \lambda_K \|\text{div}_x(\alpha \nabla_x v)\|_{L_2(K)}^2 \big]. \tag{8}$$

We mention that both norms are not only well defined on the IGA space $V_{0h}$ but also on the extended space $V_{0h,*} = V_{0h} + H_0^{L,1}(Q)$ to which the solution $u$ belongs in the maximal parabolic regularity setting considered here. The Galerkin orthogonality directly follows from subtracting (6) from (4). The proof of the other two properties is also elementary; see [10, 11].

From the $V_{0h}$-coercivity of the bilinear form $a_h(\cdot,\cdot)$, we conclude that the solution $u_h$ of the IGA scheme (6) is unique, and, therefore, it exists. In other words, the corresponding linear system of IGA equations

$$K_h \underline{u}_h = \underline{f}_h \tag{9}$$

has a unique solution $\underline{u}_h = (u_i)_{i=1}^{N_h} \in \mathbb{R}^{N_h = |\mathcal{I}_0|}$. The coefficients (control points) $u_i$ then uniquely define the solution $u_h = \sum_{i=1}^{N_h} u_i \varphi_i$ of the IGA scheme (6). The system matrix $K_h$ is non-symmetric, but positive definite due to the $V_{0h}$-coercivity.

The following best-approximation estimate directly follows from properties 1. - 3. given above:

**Theorem 1** *Let $u \in U_0 \cap H_0^{L,1}(Q)$ be the solution of the IBVP* (2)*, and $u_h \in V_{0h}$ the solution of space-time IGA schemes* (6)*. Then the best-approximation estimate*

$$\|u - u_h\|_h \le \inf_{v_h \in V_{0h}} \left( \|u - v_h\|_h + \frac{\mu_b}{\mu_c} \|u - v_h\|_{h,*} \right) \tag{10}$$

*holds.*

The best-approximation estimate (10) finally yields convergence rate estimates in terms of $h$ respectively the local mesh-sizes $h_K$, $K \in \mathcal{K}_h$, provided that $u$ has some additional regularity; see [10, 11].

In practical application, the use of adaptive IGA schemes is more attractive than uniform mesh refinement. In order to drive adaptivity, we need local error indicators, a marking strategy, and the possibility to refine the mesh locally. In IGA, which starts from a tensor-product setting, local mesh refinement is more involved than in the FEM. However, nowadays, several refinement techniques are available; see [10] and the references given therein. Local error indicators $\eta_K(u_h)$, $K \in \mathcal{K}_h$, should be derived from a posteriori error estimators. We here consider functional error estimators that provide an error bound for any conform approximation $v$ to the solution $u$ of (2). Of course, we are interested in the case $v = u_h \in V_{0h}$. We get the following functional error estimator for a special choice of parameters from [18]:

$$|||u - u_h|||^2 \le \overline{\mathfrak{M}}^2(\beta, u_h, \mathbf{y}) := \sum_{K \in \mathcal{K}_h} \eta_K^2(\beta, u_h, \mathbf{y}), \tag{11}$$

where the norm is defined by $|||w|||^2 := \|\sqrt{\alpha}\nabla_x w\|^2_{L_2(Q)} + \|w\|^2_{L_2(\Sigma_T)}$, $\beta$ is a fixed positive scaling parameter (function [18]), and $\mathbf{y} \in H(\mathrm{div}_x, Q)$ is a suitable flux reconstruction. The local error indicator $\eta_K^2(\beta, u_h, \mathbf{y}) := \eta_{K,\mathrm{flux}}^2(\beta, u_h, \mathbf{y}) + \eta_{K,\mathrm{pde}}^2(\beta, u_h, \mathbf{y})$ consists of the parts

$$\eta_{K,\mathrm{flux}}^2(\beta, u_h, \mathbf{y}) := \int_K (1+\beta)|\mathbf{y} - \alpha\nabla_x u_h|^2 dK \quad \text{and} \tag{12}$$

$$\eta^2_{K,\mathrm{pde}}(\beta,u_h,\mathbf{y}) := c^2_{F\Omega}\int_K \left(\frac{1+\beta}{\beta}|f-\partial_t u_h+\mathrm{div}_x\mathbf{y}|^2\right)dK \tag{13}$$

evaluating the errors in the flux and in the residual of the PDE, where $c_{F\Omega}$ denotes the constant in the inequality $\|v\|_{L_2(Q)} \le c_{F\Omega}\,\|\sqrt{\alpha}\nabla_x v\|_{L_2(Q)}$ for all $v \in V$. For $\alpha = 1$, $c_{F\Omega}$ is nothing but the Friedrichs constant in $H^1_0(\Omega)$. In contrast to the FEM (see Sect. 4), the IGA flux $\alpha\nabla_x u_h$ belongs to $H(\mathrm{div}_x, Q)$ provided that $\alpha$ is sufficiently smooth, and $V_{0h} \subset C^1(\overline{Q})$ that is ensured for $k \ge 2$. Then we can choose $\mathbf{y} = \alpha\nabla_x u_h$ yielding $\eta_{K,\mathrm{flux}}(\beta,u_h,\mathbf{y}) = 0$ and, therefore, $\eta_K(\beta,u_h,\mathbf{y}) = \eta_{K,\mathrm{pde}}(\beta,u_h,\mathbf{y})$. A more sophisticated flux reconstruction was proposed by Kleiss and Tomar for elliptic boundary value problems in [8]. Following this idea, we also propose to reconstruct the flux $\mathbf{y}$ from the minimization of the majorant $\overline{\mathfrak{M}}^2(\beta,u_h,\mathbf{y})$ in an IGA space $(\mathcal{S}^l_{l-1,H})^d$ on a coarser mesh with some mesh-size $H \ge h$ and with smoother splines of the underlying degree $l \ge k$. In [10, 11], we present and discuss the results of many numerical experiments showing the efficiency of this technique for constructing adaptive space-time IGA methods using different marking strategies. Here we only show an example from [1] with the manufactured solution $u(x,t) = x^{5/2}(1-x)t^{3/4}$ of (1) with $Q = (0,1)\times(0,2)$, $\alpha = 1$, and $\mathbf{f} = 0$. The uniform mesh refinement yields $O(h^{3/4})$ in the $\|\cdot\|_h$ norm for $k = 2$, whereas the adaptive version with THB-splines recovers the full rate $O(h^2)$, where $h = N_h^{-2}$ and $k = 2$; see Fig. 1.

## 4 Space-Time Finite Element Analysis

We can construct locally stabilized space-time finite element schemes in the same way as in the IGA case replacing the IGA space (3) by the finite element space

$$V_{0h} = \{v_h \in C(\overline{Q}) : v_h(x_K(\cdot)) \in \mathbb{P}_k(\hat{K}),\ \forall K \in \mathcal{K}_h,\ v_h = 0 \text{ on } \overline{\Sigma}\cap\overline{\Sigma}_0\}, \tag{14}$$

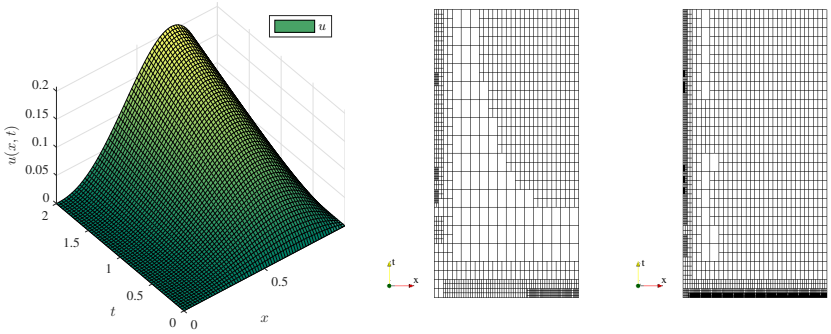


**Fig. 1:** Solution $u(x,t)$ (right), mesh after 6 (middle) and 8 (right) adaptive refinement levels.

where $\mathcal{K}_h$ is a shape regular decomposition of the space-time cylinder $Q$ into simplicial elements, i.e., $\overline{Q} = \bigcup_{K \in \mathcal{K}_h} \overline{K}$, and $K \cap K' = \emptyset$ for all $K$ and $K'$ from $\mathcal{K}_h$ with $K \neq K'$ (see, e.g., [3] for details), $x_K(\cdot)$ denotes the map from the reference element $\hat{K}$ (unit simplex) to the finite element $K \in \mathcal{K}_h$, and $\mathbb{P}_k(\hat{K})$ is the space of polynomials of the degree $k$ on the reference element $\hat{K}$. For the space-time finite element solution $u_h \in V_{0h}$ of (6), we can derive the same best-approximation estimate as given in Theorem 1, from which we get convergence rate estimates under additional regularity assumptions; see [13, Theorem 13.3]. The case of special distributional sources $\mathbf{f}$, the divergence of which exists in $L_2(Q_i)$ on subdomains $Q_i$ of a non-overlapping domain decomposition of the space-time cylinder $\overline{Q} = \bigcup_{i=1}^{m} \overline{Q}_i$, and the case of low-regularity solutions are investigated in [14]. In [13] and [14], we also present numerical results for different benchmark examples exhibiting different features in space and time. We compare uniform and adaptive refinement. In the finite element case, the corresponding system (9) of algebraic equations is always solved by a parallel AMG preconditioned GMRES. We use *BoomerAMG*, provided by the linear solver library hypre[1], to realize the AMG preconditioner. The adaptive version can be based on different local error indicators; see [13, 14]. Below we show an example where we compare uniform refinement with the adaptive refinement that is based on Repin's first functional error estimate (11). It was already mentioned in Sect. 3 that, in the FEM, we cannot take $\mathbf{y} = \alpha \nabla_x u_h$ because the finite element flux does not belong to $H(\mathrm{div}_x, Q)$. Therefore, we first recover an appropriate flux $\mathbf{y}_h = R_h(\alpha \nabla_x u_h) \in (V_h)^d \subset H(\mathrm{div}_x, Q)$ by nodal averaging à la Zienkiewicz and Zhu (ZZ). One can use this $\mathbf{y}_h$ as $\mathbf{y}$, or one can improve this $\mathbf{y}_h$ by preforming some CG minimization steps on the majorant $\overline{\mathfrak{M}}^2(\beta, u_h, \mathbf{y})$ in $(V_h)^d$ with the initial guess $\mathbf{y}_h$. Finally, one minimizes with respect to $\beta$. We mention that the local ZZ-indicator is nothing but $\eta_{K,\mathrm{flux}}(0, u_h, R_h(\alpha \nabla_x u_h))$.

Let us now consider the parabolic NIST Benchmark *Moving Circular Wave Front*[2] for testing our adaptive locally stabilized space-time fe method. We again consider the parabolic IBVP (1) with the following data: $d = 2$, $Q = (0, 10) \times (-5, -5) \times (0, T) \subset \mathbb{R}^3$, $T = 10$, $\alpha = 1$, $\mathbf{f} = \mathbf{0}$, and the manufactured exact solution

$$u(x,t) = (x_1 - 0)(x_1 - 10)(x_2 + 5)(x_2 - 5) \tan^{-1}(t) \left( \frac{\pi}{2} - \tan^{-1}(\zeta(r - t)) \right) / C$$

with $r = \sqrt{(x_1 - x_{1c})^2 + (x_2 - x_{2c})^2}$, where the parameters $(x_{1c}, x_{2c})$ and $\zeta$ describe the center and the steepness of the circular wave front, respectively. We choose $(x_{1c}, x_{2c}) = (0, 0)$ and $\zeta = 20$ (mild wave front). The scaling parameter $C$ is equal to 10000. The space-time adaptivity is driven by the local error indicators $\eta_{K,\mathrm{flux}}(\beta, u_h, \mathbf{y}_h)$ using Dörfler's marking. Fig. 2 shows the adaptive meshes after a cut through the space-time cylinder $Q$ at $t = 0, 2.5, 5, 7.5$, and 10. In Fig. 3, we compare the convergence history for uniform and adaptive refinements for the polynomial degrees $k = 1, 2, 3$. In the adaptive case, we use Dörfler's marking with the bulk parameter 0.25. The solution has steep gradients in the neighborhood of

[1] https://computing.llnl.gov/projects/hypre

[2] https://math.nist.gov/cgi-bin/amr-display-problem.cgi

the wave front that is perfectly captured by the adaptive procedure. This adaptive procedure quickly leads to the optimal rates $O(h^k)$, and dramatically reduces the error in the $\|\cdot\|_h$ norm, where $h = (N_h)^{-1/(d+1)} = N_h^{-1/3}$ in the adaptive case. Fig. 4 shows the corresponding efficiency indices $I_{\text{eff}} = \eta_{\text{flux}}(0, u_h, \mathbf{y}_h)/\|u - u_h\|_h$, where $\eta^2_{\text{flux}}(\beta, u_h, \mathbf{y}_h) = \sum_{K \in \mathcal{K}_h} \eta^2_{K,\text{flux}}(\beta, u_h, \mathbf{y}_h)$.

## 5 Space-Time Optimal Control

The optimal control of evolution equations turns out to be interesting from both a mathematical and a practical point of view. Indeed, there are many important applications in technical, natural, and life sciences. Let us first consider the following space-time tracking optimal control problem: For a given target function $u_d \in L_2(Q)$ (desired state) and for some appropriately chosen regularization (cost) parameter $\varrho > 0$, find the state $u \in U_0$ and the control $z \in Z$ minimizing the cost functional

$$J(u, z) = \frac{1}{2} \int_Q |u - u_d|^2 \, \mathrm{d}Q + \frac{\varrho}{2} R(z) \tag{15}$$

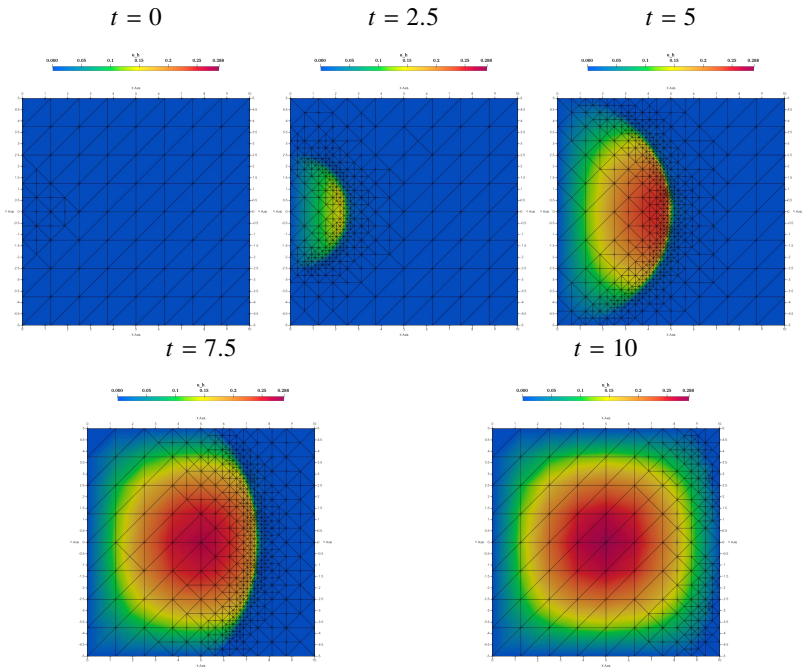


**Fig. 2:** Adaptive space-time meshes at the cuts $t = 0, 2.5, 5, 7.5$, and 10 through $Q \subset \mathbb{R}^3$.

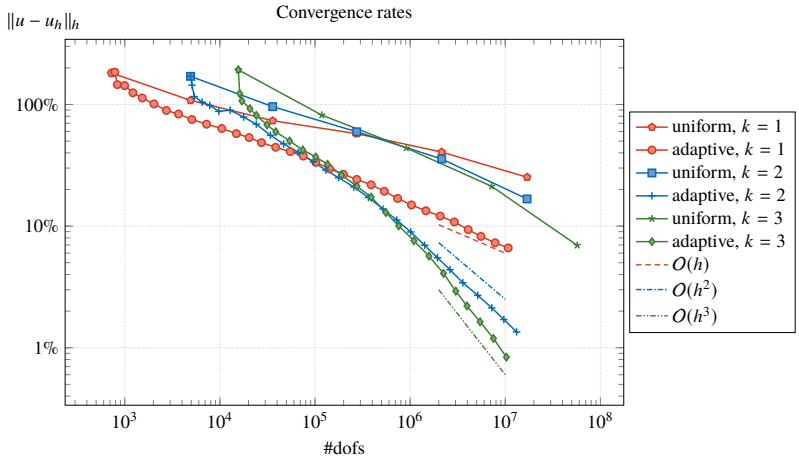


**Fig. 3:** Comparison of uniform and adaptive refinements for $k = 1, 2, 3$.

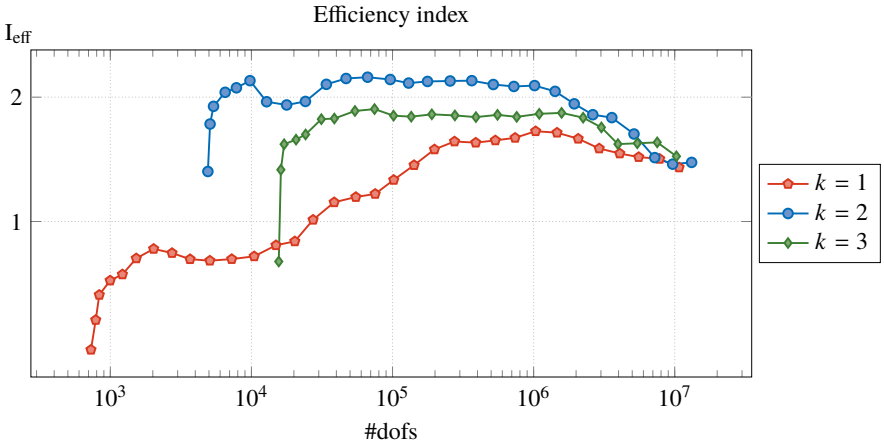


**Fig. 4:** Efficiency indices $I_{\text{eff}}$ for Dörfler's marking with bulk parameter 0.25

subject to the linear parabolic IBVP (1) respectively its variational formulation (2). The regularization term $R(z)$ is usually chosen as the $L_2(Q)$-norm $\|z\|^2_{L_2(Q)}$, and, thus, $Z = L_2(Q)$, whereas the control $z$ acts as right-hand side $f$ in (1) respectively (2), and $\mathbf{f} = \mathbf{0}$. Since the state equation (2) has a unique solution $u \in U_0$, one can reason the existence of a unique control $z \in Z$ minimizing the quadratic cost functional $J(S(z), z)$, where $S$ is the solution operator mapping $z \in Z$ to the unique solution $u \in U_0$ of (2); see, e.g., [17] and [21]. On the other side, the solution of the quadratic optimization problem $\min_{z \in Z} J(S(z), z)$ is equivalent to the solution of the first-order optimality system. After eliminating the control $u$ from the optimality

system by means of the gradient equation $p + \varrho z = 0$, we arrive at the reduced optimality system: Find the state $u \in U_0$ and the adjoint state $p \in P_T$ such that

$$\begin{aligned} \varrho \int_Q \Big[\partial_t u\, v + \alpha\, \nabla_x u \cdot \nabla_x v\Big] dQ + \int_Q p\, v\, dQ = 0, \\ - \int_Q u\, q\, dQ + \int_Q \Big[ - \partial_t p\, q + \alpha\, \nabla_x p \cdot \nabla_x q\Big] dQ = - \int_Q u_d\, q\, dQ, \end{aligned} \tag{16}$$

holds for all $v, q \in V$, where $P_T := \{p \in W(0,T) : p = 0 \text{ on } \Sigma_T\}$. Now the well-posedness of (16) can again be proved by means of the BNB theorem verifying the corresponding conditions (BNB1) – (BNB3); see [16, Theorem 3.3]. In the same paper, we analyze the finite element Galerkin discretization of the reduced optimality system: Find $(u_h, p_h) \in U_{0h} \times P_{Th}$ such that

$$B(u_h, p_h; v_h, q_h) = -(u_d, q_h)_{L_2(Q)} \quad \forall (v_h, q_h) \in V_{0h} \times V_{Th}, \tag{17}$$

where the bilinear form $B(\cdot,\cdot)$ results from adding the left-hand sides of (16). The finite element subspace spaces $U_{0h} = V_{0h} = S_h^k(Q) \cap U_0$ and $P_{Th} = V_{Th} = S_h^k(Q) \cap P_T$ are defined on a shape-regular decomposition of the space-time cylinder $Q$ in simplicial elements as usual; cf. Section 4. Of course, we can here also use IGA instead of FEM as discretization method; cf. Section 3. In [16], we show a *discrete inf-sup condition* which leads to a best-approximation error estimate of the form

$$\sqrt{\varrho \|u - u_h\|_V^2 + \|p - p_h\|_V^2} \le c \inf_{(v_h, q_h) \in U_{0h} \times P_{Th}} \sqrt{\|u - v_h\|_{U_0}^2 + \|p - q_h\|_{P_T}^2} \tag{18}$$

for the case $\alpha = 1$, where $c = 1 + 2\sqrt{2} c_B(\varrho)$ and $c_B(\varrho)$ is the boundedness constant of the bilinear form $B(\cdot,\cdot)$. If $u$ and $p$ have additional regularity, we easily get convergence rate estimates, e.g., $O(h)$ if $u, p \in H^2(Q)$; see [16, Theorem 3.5].

In some applications, one wants to restrict the action of the control $z$ in space and time. Thus, in the case of partial control, we have to replace the right-hand side $f = z$ by $f = \chi_{Q_c} z$, where $\chi_{Q_c}$ is the characteristic function of the space-time control domain $Q_c \subset Q$. Then we can again derive the reduced optimality system, and solve it by means of the space-time finite element method. Let us consider a concrete example. In this example, we consider the spatial domain $\Omega = (0,1)^2$ and the terminal time $T = 1$. Therefore, we have $Q = (0,1)^3$. The control subdomain is given as $Q_c = (0.25, 0.75)^2 \times (0,T)$. A smooth target $u_d = \sin(\pi x)\sin(\pi y)\sin(\pi t)$ is used, and the regularization (cost) parameter $\varrho = 10^{-5}$. Fig. 5 presents the state $u_h$ and the control $z_h$ for partial (up) and full (down) distributed controls. We use continuous, piecewise linear finite element approximations on a quasi-uniform decomposition of $Q$ into tetrahedral elements.

Finally, we mention that, in [15], we introduce and investigate the space-time energy regularization $R(z) = \|z\|^2_{L_2(0,T;H^{-1}(\Omega))}$, and compare it to the $L_2(Q)$ and the sparse regularization. Furthermore, the space-time approach can easily be generalized to other observations like terminal time observation, the control via boundary conditions, the control via initial conditions (inverse heat conduction problem), and,

last but not least, the control of non-linear parabolic IBVP with box constraints imposed on the control [16].

**Acknowledgements** The author would like to thank his coworkers mentioned in the *Introduction* for the collaboration on finite element and isogeometric space-time methods. Furthermore, this research was supported by the Austrian Science Fund (FWF) through the projects NFN S117-03 and DK W1214-04. This support is gratefully acknowledged.

## References

1. Devaud, D., and Schwab, C. Space–time hp-approximation of parabolic equations. *Calcolo 55*, 3 (2018), 1–23.
2. Dier, D. Non-autonomous maximal regularity for forms of bounded variation. *J. Math. Anal. Appl. 425* (2015), 33–54.
3. Ern, A., and Guermond, J.-L. *Theory and Practice of Finite Elements*. Springer, NY, 2004.

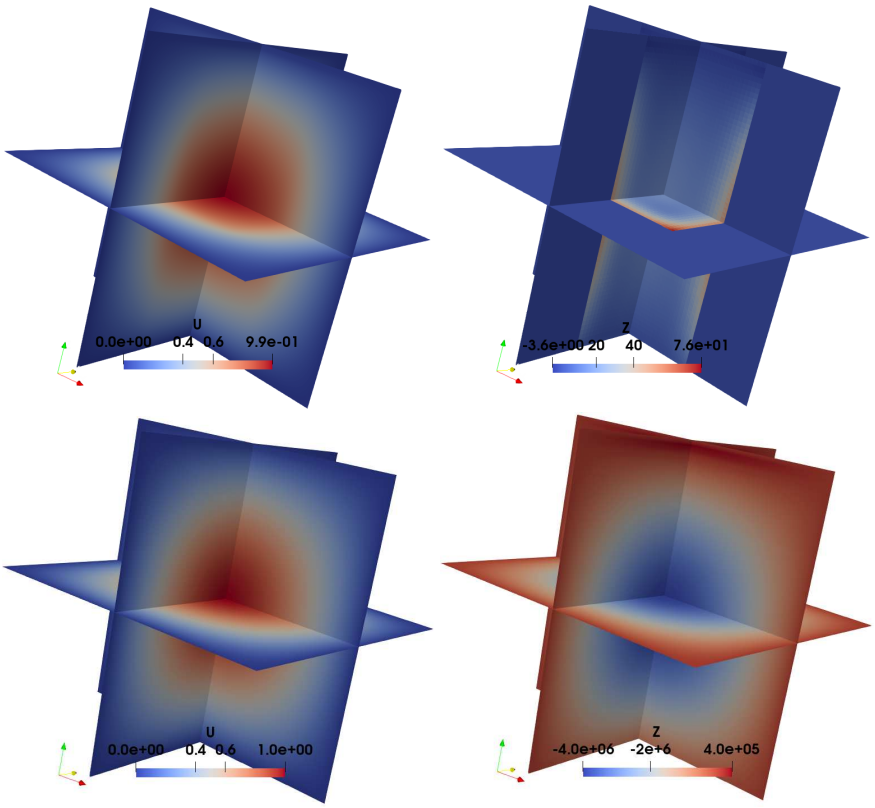


**Fig. 5:** The state $u$ (left) control $z$ (right) for partial control (up) and full control (down).

4. Hughes, T., and Brooks, A. A multidimensional upwind scheme with no crosswind diffusion. In *Finite Element Methods for Convection Dominated Flows* (New York, 1979), T. Hughes, Ed., vol. 34 of *AMD*, ASME.
5. Hughes, T., Cottrell, J., and Bazilevs, Y. Isogeometric analysis: CAD, finite elements, NURBS, exact geometry and mesh refinement. *Comput. Methods Appl. Mech. Engrg. 194* (2005), 4135–4195.
6. Hughes, T., Franca, L., and Hulbert, G. A new finite element formulation for computational fluid dynamics: VIII. The Galerkin/least-squares method for advection-diffusive equations. *Comput. Methods Appl. Mech. Engrg. 73* (1989), 173–189.
7. Johnson, C., and Saranen, J. Streamline diffusion methods for the incompressible Euler and Navier-Stokes equations. *Math. Comp. 47*, 175 (1986), 1–18.
8. Kleiss, S., and Tomar, S. Guaranteed and sharp a posteriori error estimates in isogeometric analysis. *Comput. Math. Appl. 70*, 3 (2015), 167–190.
9. Ladyžhenskaya, O. *The boundary value problems of mathematical physics*, vol. 49 of *Applied Mathematical Sciences*. Springer-Verlag, New York, 1985.
10. Langer, U., Matculevich, S., and Repin, S. Adaptive space–time Isogeometric Analysis for parabolic evolution problems. In *Space–Time Methods: Applications to Partial Differential Equations*, U. Langer and O. Steinbach, Eds., vol. 25 of *Radon Series on Computational and Applied Mathematics*. de Gruyter, Berlin, 2019, pp. 155–200.
11. Langer, U., Matculevich, S., and Repin, S. Guaranteed error bounds and local indicators for adaptive solvers using stabilised space-time IgA approximations to parabolic problems. *Comput. Math. with Appl. 78* (2019), 2641–2671.
12. Langer, U., Moore, S., and Neumüller, M. Space-time isogeometric analysis of parabolic evolution equations. *Comput. Methods Appl. Mech. Engrg. 306* (2016), 342–363.
13. Langer, U., Neumüller, M., and Schafelner, A. Space-time finite element methods for parabolic evolution problems with variable coefficients. In *Advanced Finite Element Methods with Applications - Selected Papers from the 30th Chemnitz Finite Element Symposium 2017*, T. Apel, U. Langer, A. Meyer, and O. Steinbach, Eds., vol. 128 of *LNCSE*. Springer, Berlin, Heidelberg, New York, 2019, ch. 13, pp. 247–275.
14. Langer, U., and Schafelner, A. Adaptive space-time finite element methods for non-autonomous parabolic problems with distributional sources. *Comput. Methods Appl. Math. 20*, 4 (2020), 677–693.
15. Langer, U., Steinbach, O., Tröltzsch, F., and Yang, H. Space-time finite element discretization of parabolic optimal control problems with energy regularization. *SIAM J. Numer. Anal. 59*, 2 (2021), 660–674.
16. Langer, U., Steinbach, O., Tröltzsch, F., and Yang, H. Unstructured space-time finite element methods for optimal control of parabolic equation. *SIAM J. Sci. Comput. 43*, 2 (2021), A744–A771.
17. Lions, J. *Optimal control of systems governed by partial differential equations.*, vol. 170. Springer, Berlin, 1971.
18. Repin, S. *A posteriori estimates for partial differential equations*, vol. 4 of *Radon Series on Computational and Applied Mathematics*. de Gruyter, Berlin, 2008.
19. Steinbach, O. Space-time finite element methods for parabolic problems. *Comput. Methods Appl. Math. 15*, 4 (2015), 551–566.
20. Thomée, V. *Galerkin finite element methods for parabolic problems*, second ed., vol. 25 of *Springer Series in Computational Mathematics*. Springer-Verlag, Berlin, 2006.
21. Tröltzsch, F. *Optimal control of partial differential equations: Theory, methods and applications*. American Mathematical Society, Providence, Rhode Island, 2010.